



Available online at [scholarcommons.usf.edu/ijis](https://scholarcommons.usf.edu/ijis)

# International Journal of Speleology

Official Journal of Union Internationale de Spéléologie



## Role of hypogenesis in the evolution of karst in the Taurus Mountains Range, Turkey

C. Serdar Bayarı <sup>1\*</sup>, N. Nur Özyurt <sup>1</sup>, Lütfi Nazik <sup>2,3</sup>, Koray A. Törk <sup>3</sup>,  
İ. Noyan Güner <sup>4</sup>, Emrah Pekkan <sup>5</sup>, and Pınar Avcı <sup>1</sup>

<sup>1</sup>Department of Geological Engineering, Hydrogeological Engineering Section, Hacettepe University, Beytepe 06800 Ankara, Turkey

<sup>2</sup>Department of Geography, Ahi Evran University, Merkez 40100 Kırşehir, Turkey

<sup>3</sup>Karst and Cave Research Unit, General Directorate of Mineral Exploration and Research, Çankaya 06530 Ankara, Turkey

<sup>4</sup>Hydrogeological Applications Unit, General Directorate of Mineral Exploration and Research, Çankaya 06530 Ankara, Turkey

<sup>5</sup>Institute of Earth and Space Sciences, Eskişehir Technical University, Tepebaşı 26555 Eskişehir, Turkey

**Abstract:** Field observations and laboratory data collected from the Taurus Mountains Range, Turkey during the last two decades provided evidence for the link between the evolution of hypogene karst and the geodynamic history. Major evidence includes; carbonate-hosted secondary ore deposits that are converted from primarily hypogene minerals by epigene, oxygen-rich groundwater circulating at local to intermediate depths. Another piece of evidence of hypogene karst in the Tauride is the Kırkgöz Springs' huge submerged cave/conduit system, which formed the Antalya Travertine Plateau, which is the world's largest deposit precipitated by cool karst groundwater. The obruks in central Tauride are giant collapse dolines formed by ascending hypogene fluids in the upper continental crust, rich in volcanogenic carbon dioxide. The groundwater's noble gas and carbon isotope data are helpful in determining the existing but asymptomatic hypogene activity in the upper crust. Hypogene karst development seems common in parts of the world with current or past geodynamic activity. However, a hydrogeological overview of the geodynamic history is essential to assess the hypogene processes and their reflections on the land surface.

**Keywords:** Geodynamic evolution, carbonate-hosted ore, Kırkgöz springs, obruks, earth-tide

*Received 28 February 2024; Revised 8 June 2024; Accepted 11 June 2024*

**Citation:** Bayarı, C.S., Özyurt, N.N., Nazik, L., Törk, K.A., Güner, İ.N., Pekkan, E., Avcı, P., 2024. Role of hypogenesis in the evolution of karst in the Taurus Mountains Range, Turkey. *International Journal of Speleology*, 53(2), 111-128. <https://doi.org/10.5038/1827-806X.53.2.2501>

### INTRODUCTION

The Taurus Mountains Range of Turkey, which is a part of the Alpidic (or Alpine-Himalayan) Orogenic Belt, is a unique karst region on a worldwide scale because it includes different types of settings ranging from coastal-submarine to high-elevation glacial karst systems with numerous evidences of epigene and hypogene karst development.

The range is located in southern Turkey and extends from west to east for about 1,500 km, and its south-north extension varies between 150 and 350 km (Fig. 1). It is bounded by the Mediterranean Sea and Arabian Platform from the south and by the Pontide Mountains Range from the north. The Taurus Mountains Range constitutes the Tauride part of the Anatolide-Tauride tectonic unit. The Pontide, the Anatolide-Tauride, and the Arabian Platform are the main tectonic units that have combined to form the present landmass of Turkey.

Klimchouk (2017) provided a conceptual framework for the genetic categorization and discrimination of

characteristic settings of hypogene karst based on the consideration of driving forces and conditions for fluid circulation and ascending flow in the upper continental crust in the context of tectonic/geodynamic history and positions. He noticed that “an understanding of hypogene karst requires much deeper and broader hydrogeological and geodynamic context as compared to more familiar epigene karst.”

Field and laboratory data obtained from the western and central parts of the Taurus Mountains Range during the last two decades provided important evidence on the relationship between the evolution of hypogene karst and the geodynamic history of the region. This mountain range, which is a part of the Alpidic orogenic belt, is rich in carbonate formations that host some of the most prominent and large-scale examples of hypogene karst development in the world. In the following, we first summarize Klimchouk's (2017) work on the properties of the upper crust as related to hypogene karst development. Then, we present a brief geodynamic history of the Taurus Mountains

Range and later provide information on some cases of hypogene karstification in this karst belt. The cases include: a) carbonate-hosted ore deposits as an example of the relationship of hypogene karstification with metasomatism and other processes of fluid-induced transformations of rocks (e.g., Klimchouk et al., 2006b), b) Kırkgöz submerged cave system and the Antalya Travertine Plateau as an example of large scale porosity/permeability development and, associated carbonate mineral deposition due to strong volcanogenic carbon-

dioxide flux (e.g., Özyurt, 2007; Bayarı et al., 2016) c) obruks, the giant collapse dolines in central Anatolia as an example of volcanogenic setting of hypogene karst based on consideration of driving forces and conditions for fluid circulation and ascending flow in the upper continental crust (e.g., Bayarı et al., 2009a, b), d) isotope data of groundwater indicating hypogene activity in the Tauride and, e) Earth-tidal pumping as an example of a potential flow driver in deep hypogene karst systems (Bayarı et al., 2011, Bayarı & Özyurt, 2014).

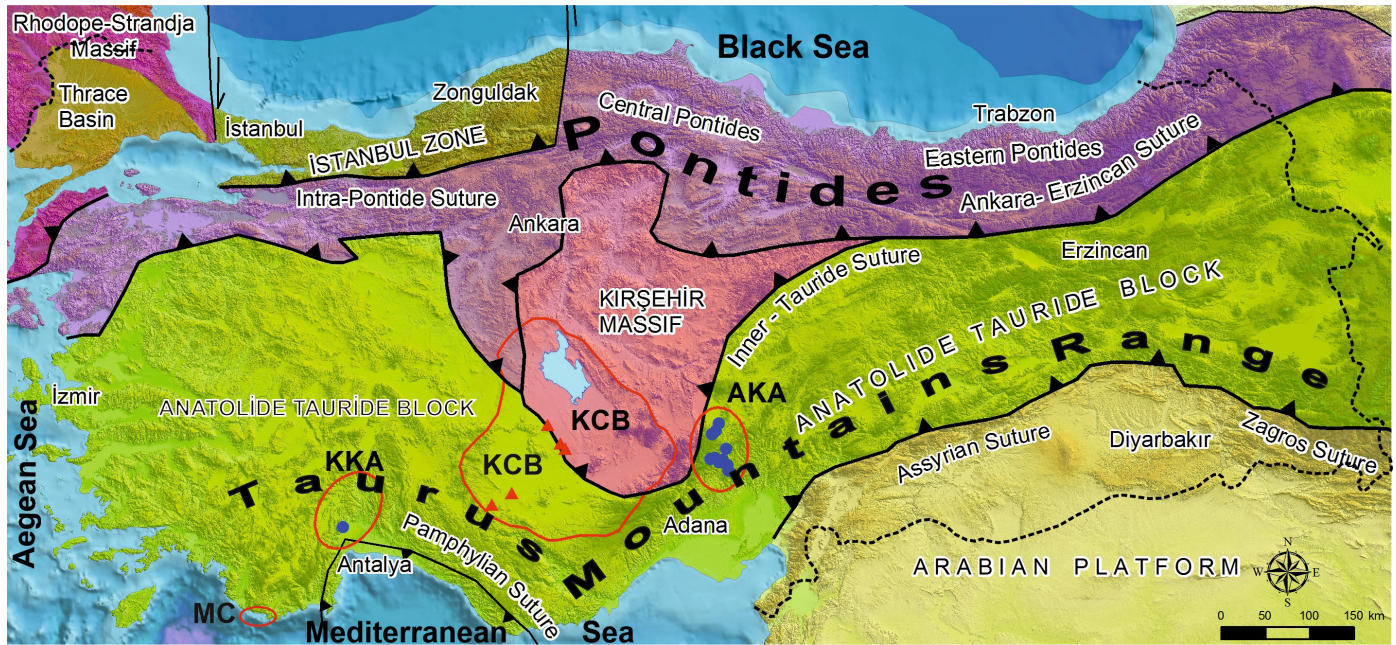


Fig. 1. Location of sites mentioned in text on the map of tectonic units of the Anatolian Plate (modified after Özyurt & Bayarı, 2014). MC: Mivini submarine cave, KKA: Kırkgöz karst aquifer, KCB: Konya Closed Basin, AKA: Aladağlar karst aquifer.

**PROPERTIES OF UPPER CONTINENTAL CRUST AS RELATED TO HYPOGENE KARST**

In his prominent paper “Types and Settings of Hypogene Karst”, Klimchouk (2017) provided “an overview of basic concepts about fluid dynamics and hydrodynamic zoning of the upper continental crust and about the

influence of mantle processes on crustal fluids.” In the following, we briefly summarize the outlines of his work in order to make the information presented in this paper easier to comprehend for the readers new to the subject. A graphical presentation of his views mentioned in our summary is given in Figure 2.

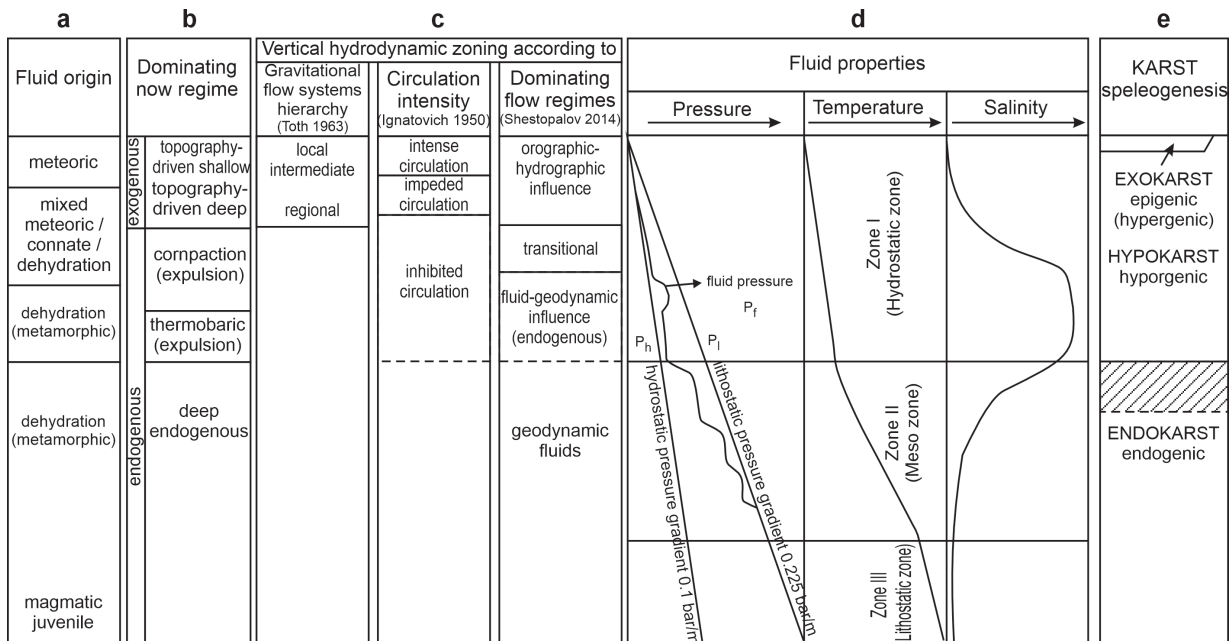


Fig. 2. Approximate reconciliation of views on (a) fluid origins, (b) flow regimes, (c) vertical hydrodynamic zoning, (d) fluid properties, and (e) vertical karst zoning in the upper continental crust (modified after Fig. 4 of Klimchouk, 2017).

The two major genetic types of karst within the upper part of the Earth's crust are epigene and hypogene. The epigene karst development is associated with interactions with the landscape, has both surface and underground components, and is driven by meteoric water. On the other hand, hypogene karst evolves exclusively by void-conduit systems at depth, without direct genetic linkage with the surface, and is driven by magmatic and metamorphic processes.

Meteoric water is derived from precipitation, and the water in the hydrological cycle is almost entirely composed of this water. The water trapped in sedimentary deposits during their formation is called connate (formation) water, which is usually paleo-seawater. Chemical reactions and mass transport in epigene karst are maintained by these types of water.

Magmatic water (i.e., juvenile or young) is released from magma during crystallization or solidification phases within the deep crust and asthenosphere. The lithostatic and tectonic pressures, along with the heat flux from the asthenosphere, result in devolatilization reactions and in metamorphism of sedimentary or magmatic rocks that release metamorphic (thermogenic) fluids, including water. Endogenous and hypogene (magmatic) karst development is driven by magmatic and/or metamorphic fluids (i.e., endogenic water). Accordingly, meteoric and connate waters may be called "exogenic water." Endogenic and exogenic waters are parts of "geological" and "hydrological" water cycles, respectively (see Fig. 1 of Klimchouk, 2017). Upward migration of aggressive endogenic waters favors hypogene karst development and the formation of sulfidic ore deposits. These deposits can turn into carbonate-hosted oxide and/or carbonate ore deposits by flushing with oxygen-rich exogenic waters of epigene origin (e.g., Haniççi et al., 2019).

According to Klimchouk (2017), the dominant fluid flow regimes in the upper continental crust are, from top to bottom: a) topography-driven shallow and deep; b) compaction-related expulsion; c) thermobaric expulsion; and d) deep endogenous. The main driver of the "topography-driven shallow and deep" regimes is the force of gravity applied to groundwater.

During diagenesis (compaction), the pressure head applied by the lithostatic (and/or tectonic) loading expels the connate (formation) water out of the pores of sediments. This type of flow regime is generally considered of limited importance for hypogene karst development because most of the connate water is lost during earlier stages of diagenesis (e.g., Klimchouk, 2017). The thermobaric regime develops at deeper burial depths where both temperature and lithostatic loading increase. Thermal expansion of water and/or mineral dehydration evolves into a highly overpressured and generally upward thermobaric flow. This deep endogenous flow regime involves fluids from metamorphism, devolatilization in the lower crust, mantle, and core and may cause endokarst development under some conditions. Karstification observed in calcareous schists in the Eastern Taurides seems to be associated with such a flow regime (e.g., Haniççi et al., 2019 and references therein).

In epigene hydrogeologic media, the groundwater flow is driven by gravity, and so the flow pattern is controlled by topographic heights of different scales (Klimchouk, 2017). This results in hierarchically nested components of local (shallow depth), intermediate (moderate depth), and regional (deep) flow systems (e.g., Toth, 1963, 2009). The distance between the recharge and discharge areas increases from local to intermediate to deep systems. According to Klimchouk (2007), "epigene karst development is largely linked with local and intermediate flow systems, often encompassing entirely upper unconfined aquifers, whereas hypogene karstification within the gravitational flow regime is associated with discharge segments of regional flow systems of the epigene karst". Klimchouk (2017) also mentions convection induced by thermal or salinity gradients (variable density flow) and seismic pumping driven by dilation and contraction in seismically active areas as other significant drivers of flow in the deep parts of sedimentary basins.

Another scheme of the intensity of groundwater circulation in the uppermost part of the crust by Ignatovich (1950) includes three zones: (1) intense circulation, (2) impeded circulation, and (3) inhibited circulation (see Fig. 2). The approach of Shestopalov (2014) to hydrodynamic zoning in the upper part of the crust distinguishes three main hydrodynamic zones: (1) orohydrographic/climatic influenced zone; (2) the intermediate (transitional) zone; (3) fluid-geodynamic influenced zone; and (4) geodynamic influenced zone (see Fig. 2). Klimchouk (2017) presents another approach to hydrodynamic zoning of the upper continental crust based on studies by Mukhin (1965) and Ezhov & Lysenin (1990). These include, from surface to depth, (a) the zone of hydrostatic pressures (Zone I), (b) the meso-zone (Zone II), and (c) the zone of lithostatic pressures (Zone III). The depth of Zone I is between 0.5 km and 7 km or more. Here the pressure is either hydrostatic or slightly (10-20%) above it. Zone II is transitional between Zone I of hydrostatic pressures above and Zone III of lithostatic pressures below. Abrupt increases in hydrostatic pressure observed in zones II and III probably originate from the increased porosity due to hydrofracturing. Lithostatic and hydrostatic pressures and temperatures increase depthwise in the exokarst, hypokarst, and endokarst sections of the upper continental crust. However, salinity, which increases in the exokarst and hypokarst sections, shows a declining trend in the endokarst section due to the release of magmatic water (Ezhov et al., 1992). This would affect the aggressivity of crustal fluids because, generally, the activity of dissolved chemical species is inversely related to salinity.

## **GEOLOGICAL EVOLUTION OF THE TAURIDE KARST BELT**

It is vital to understand the geodynamic history of the Tauride since the development of hypogene karst in the Taurus Mountains Range has been affected by the magmatism associated with plate and intraplate tectonic processes. The terranes that now comprise

Turkey's major landmass were situated in the ocean branches between the supercontinents Laurasia and Gondwana Land. These terranes were rifted off and drifted away from the supercontinents throughout the Cadomian, Variscan, Cimmerian, and Alpidic orogenic cycles (e.g., Göncüoğlu, 2019).

Geologically, Turkey consists of three main tectonic units named Pontide, Anatolide-Tauride, and Arabian Platform, which were separated from each other by the northern, and southern, branches of the Neotethys Ocean. The Pontide tectonic unit and the Anatolide-Tauride tectonic unit, along with the Arabian Platform, form the northern, southern, and southeastern parts of the Anatolian peninsula, respectively (Fig. 3).

The Anatolide-Tauride tectonic unit is a continental platform once located between the northern and southern branches of the Neotethys Ocean. It is divided into three sets of structural units. From north to south, the Kütahya-Bolkardağı Belt represents the northern edge of the platform, Anatolide

represents the metamorphic core, and the Tauride (i.e., Taurus Mountains Range), a package of mostly non-metamorphic carbonate nappes with extensive epigene and hypogene karstification, is located at the south (Göncüoğlu, 2010) (see Fig. 3). Anatolia (or Asia Minor) is a peninsula surrounded by the Black Sea and Marmara Sea to the north, and the Aegean Sea to the west, and the Mediterranean Sea to the south. Anatolia took the form of a single landmass in the Oligocene as a result of the collision of different terranes, which consisted of several island arcs or continental strips separated by relatively narrow oceanic seaways (branches) of the Neotethys ocean during the Alpidic (or Alpine-Himalayan or the Tethyan) orogeny (Okay, 2008). The ophiolite and accretionary complexes scattered throughout Turkey are remnants of these ocean branches. More elaborate information on the geodynamic history of Tauride since Neoproterozoic can be found in several benchmark papers (e.g., Özgül, 1976, 1984; Okay, 2008; Göncüoğlu, 2019).

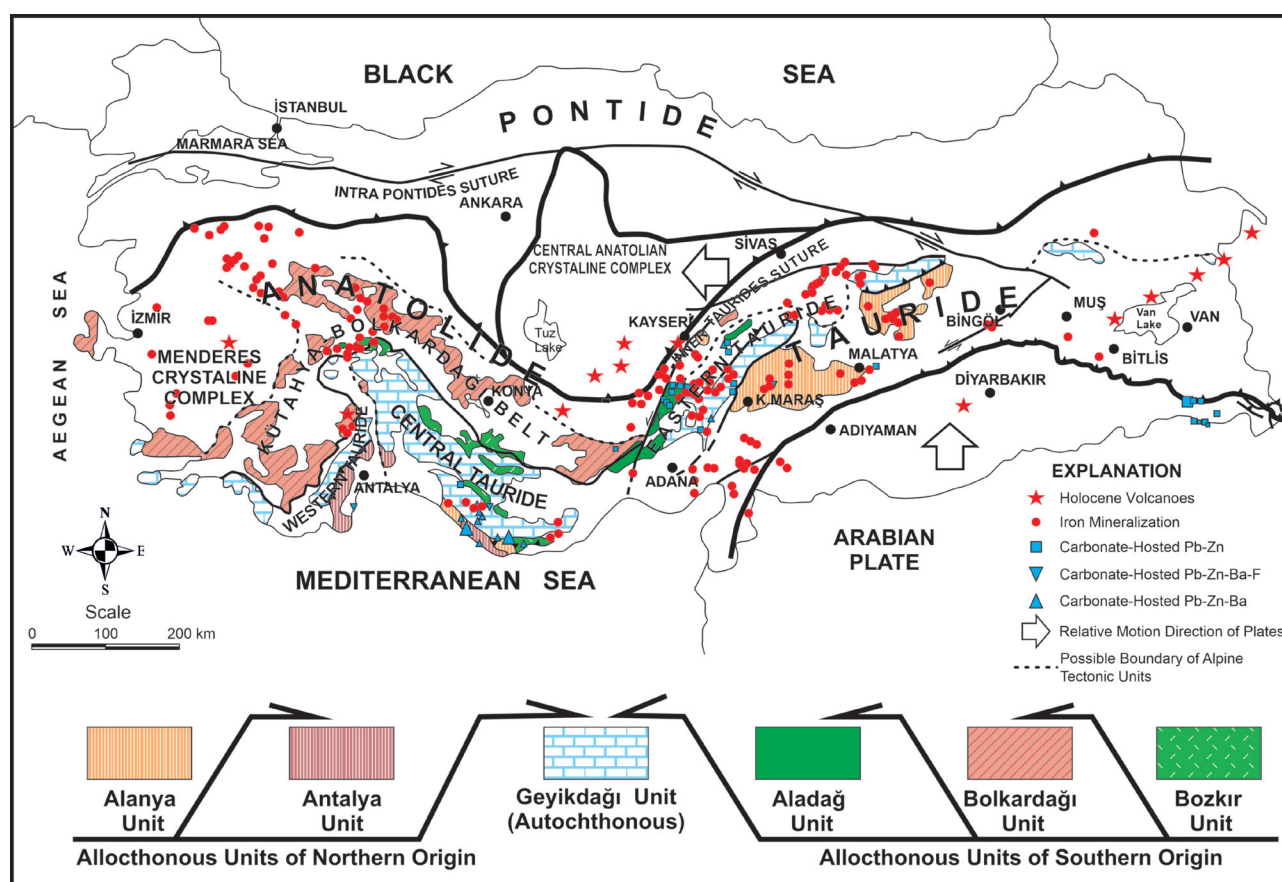


Fig. 3. Geographic distribution and tectonic positions of the autochthonous and allochthonous units of the Taurus Mountains Range (the nomenclature of tectonic units is from Özgül, 1976, 1984; Göncüoğlu et al., 1997; Ophiolite Belts Nomenclature: Juteau, 1980; Possible Limit of Alpine Tectonic Units: Göncüoğlu et al., 1997; Göncüoğlu, 2010; modified after Haniççi et al., 2019 and Hozatlıoğlu et al., 2020).

### Geodynamic evolution of the Anatolide-Tauride Terrane

The Anatolide-Tauride terrane (also called a tectonic unit or platform) experienced Alpidic deformation and regional metamorphism during the late Cretaceous and Paleocene phases of obduction, subduction, and continental collision. A massive ophiolite mass and underlying ophiolitic mélangé tectonic slices were emplaced over the Anatolide-Tauride tectonic unit during the Middle Cretaceous. At depths of more than 70 km beneath this oceanic thrust sheet,

the northern edge of the Anatolide-Tauride terrane experienced a HP/LT (high pressure/low temperature) metamorphism. Paleocene was the beginning of a continental collision between the Anatolide-Tauride and Pontide terranes, which caused the Anatolide-Tauride terrane to be internally sliced, producing a thrust pile that was oriented toward the south or southeast. This obduction lasted until the early-middle Miocene in western Turkey. Large cover nappes comprising the tectono-stratigraphic units of the Tauride have formed in the upper portions of the

thrust pile in the south, whereas the lower portions in the north have experienced regional metamorphism.

The Anatolide represents the metamorphic northern margin of the Tauride-Anatolide Platform and consists of two large crystalline complexes: the Menderes Massif to the west and the Central Anatolian Crystalline Complex (CACC) to the east. The Tauride starts with a HP/LT metamorphic peripheral belt (the Kütahya-Bolkardağı Belt, KBB), which corresponds to the allochthonous Bozkır and Bolkardağ units of Özgül (1976; 1984). The KBB is observed as nappes on the northern flank of the Tauride (i.e., Taurus Mountains Range). The Taurus Mountains Range consists of a stack of thrust sheets involving various tectono-stratigraphic units. The topmost portion of the thrust sequence is often the ophiolite nappe and/or ophiolitic mélangé, which forms enormous isolated masses along the Taurus Mountains Range.

### Tectono-stratigraphic units of the Tauride Karst Belt

The tectono-stratigraphic units in the Tauride, which are barely 150 km wide now, reveal a platform that was over 1,000 km wide prior to the late Cretaceous closure of the Neotethys. This subduction resulted in a double-verging napped structure, which consists of a number of tectono-stratigraphic units with characteristic stratigraphic and structural features representing different depositional environments in the Tauride part of the Anatolide-Tauride Platform. A palinspastic reconstruction of the units utilizing their relative tectonic context and stratigraphic similarities produces the following order from north to south: Bozkır, Bolkar Dağı, Aladağ, Geyik Dağı, Antalya, and Alanya units (Özgül, 1976, 1984) (Fig. 4). Among these, Geyik Dağı Unit is regarded as an autochthonous base

that was overthrust by Aladağ, Bolkardağı, and Bozkır Units from the north and Antalya and Alanya Units from the south (Fig. 4).

During the Paleozoic, two epicontinental seas of the Neotethys Ocean existed to the north and south of Geyik Dağı Unit. The Aladağ, Bolkar Dağı, and Bozkır units formed in the northern basins and, Antalya and Alanya units formed in the southern seas, respectively (Fig. 4). The Geyik Dağı Unit experienced terrestrial conditions, favoring epigene karstification during most of the Silurian-Permian interval.

Geyik Dağı Unit consists of platform-type sediments, starting with an unmetamorphosed Lower Paleozoic basement of Infracambrian (?), Cambrian, and Ordovician rocks and a transgressive Mesozoic-Lower Tertiary sedimentary section that is made up largely of carbonates (e.g., Özgül, 1984). Stratigraphic unconformities between formations, a major stratigraphic lacuna between the Lower Paleozoic and Mesozoic, terrestrial formations, bauxite horizons, and basal conglomerates indicate a regional uplift above sea level in the Cenomanian-Senonian interval, which indicates the presence of favorable conditions for epigene karst development. The carbonate-hosted iron, lead, zinc, and barium deposits located in the Lower Cambrian and Permian formations show that the unit was also affected by hypogene processes (Fig. 10.3 of Hanilçi et al., 2019). According to Hanilçi & Öztürk (2011), the primary MVT-type deposits were associated with the late Cretaceous-Paleocene closure of the Neotethys Ocean and were formed during a transition from an extensional to a compressional regime. Paleogene nappes, which often limit ore body exposure, suggest that ore formation occurred prior to the Paleocene.

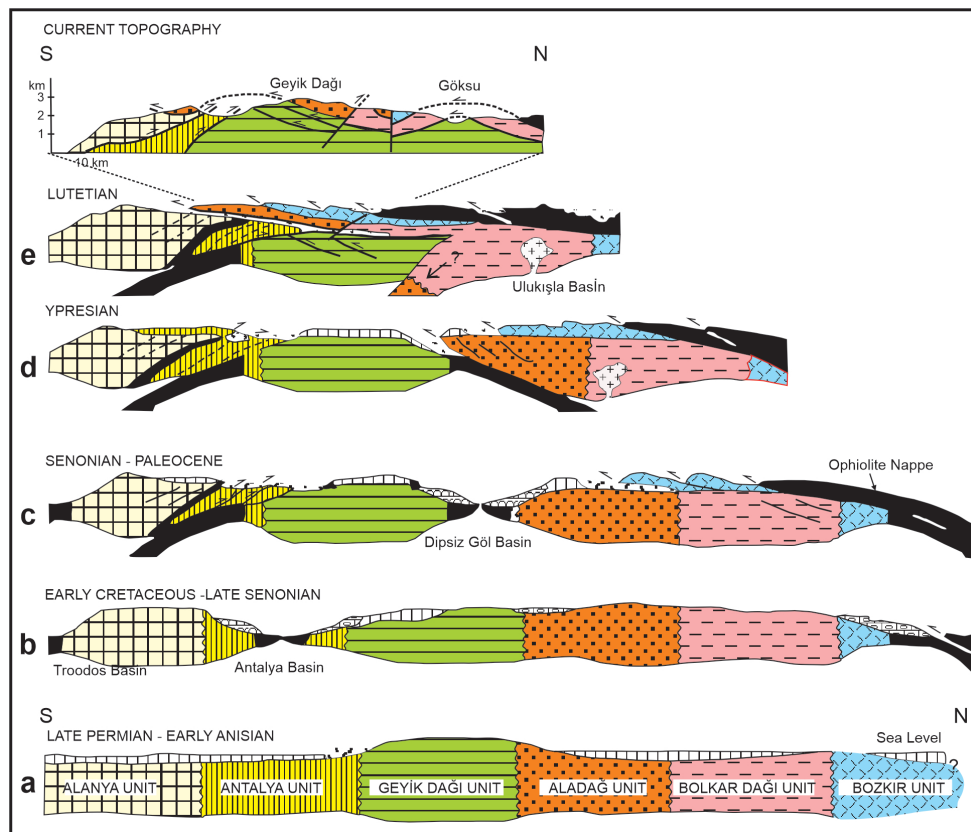


Fig. 4. Geodynamic evolution of the tectono-stratigraphic units of the Tauride (modified after Özgül, 1984).

Aladağ Unit, comprising shelf-type clastics and carbonates of the Upper Devonian-Upper Cretaceous period (e.g., Özgül, 1984). The continuous sedimentation is represented by shallow, epicontinental marine clastics and carbonates, except for a short period of uplift above sea level at the beginning of the Upper Triassic. Sulfidic and carbonate-hosted lead-zinc deposits are observed in the Lower Devonian to Upper Triassic limestones and dolomitic limestones (see Fig. 10.3 of Haniççi et al., 2019 and references therein). As in the case of the Geyik Dağı Unit, the primary ore production and the associated hypogene karst development in the Aladağ Unit seem to have occurred prior to the Paleogene. The conversion of initial sulfidic minerals to carbonate hosted deposits by epigene karst processes initiated after the Oligo-Miocene when the Taurus Mountains Range emerged.

Bolkar Dağı Unit, comprising shelf-type clastics and carbonates of the Devonian to Upper Cretaceous periods, shows regional metamorphism in greenschist facies (e.g., Özgül, 1984). The degree of metamorphism increases towards the Anatolides (i.e., crystalline complexes) and to stratigraphically deeper levels. This unit, which is intruded by plutonic rocks, also hosts lead, zinc, tin, gold, and silver deposits (e.g., Haniççi et al., 2019) associated with the geodynamic fluid circulation driven by tectonic movements and regional greenschist metamorphism.

Bozkır Unit is a melange of pelagic sediment, spilite, green tuff, diabase, ultramafic, and carbonate rock blocks of various sizes and ages spanning from the Upper Triassic to the Upper Cretaceous. Bozkır Unit tectonically overlies the Senonian olistostromes of the Aladağ and Bolkar Dağı Units and the Lutetian flysch of the Geyik Dağı Unit. Epigene karst development is observed in the carbonate rock blocks, some of which are kilometer-sized. Based on the authors' field observations, this unit does not have any evidence of hypogene karst development.

Antalya Unit comprises Lower Paleozoic and Mesozoic clastic and platform-type carbonate rocks. Well-sorted and rounded basal quartzites, local coal deposits, and stratigraphic unconformities suggest favorable conditions for epigene karst development. On the other hand, the presence of volcanic rocks and gradual recrystallization due to low-grade greenschist facies metamorphism are evidence of favorable conditions for hypogene karst development.

The Alanya Unit consists of three Permian aged metamorphic nappes, which include metaquartzite, recrystallized limestone and dolostone intercalated with pelitic schists, quartzite, garnet, micaschists with eclogite intercalations, and blueschist metabasites. The mineral composition and the rock types indicate that the unit has undergone greenschist and high-pressure/low-temperature (HP/LT) metamorphism. The Alanya Unit does not include any karstifiable rock type, but, aggressive geodynamic fluids associated with the metamorphism may have favored endogenic and hypogene karst development in the neighboring Antalya Unit, although no robust evidence exists currently.

A schematic illustration of the geodynamic evolution of the Taurides (Fig. 4) reveals that all of the views and processes (Fig. 2) associated with hypogene karst

development expressed by Klimchouk (2017) have been realized at some point in the geological past. That is, magmatic and juvenile waters were produced during intense periods of magmatism, minerals became dehydrated under conditions of metamorphism, and connate waters were released by thermobaric and compaction-related expulsions, resulting in waters of different origins, sources of depth, and circulation intensities under the effect of different dominating flow regimes involved in geodynamic evolution. While the evidence of epigene karst development can be readily observed, the hypogene karst development driven by magmatic and metamorphic processes in the void-conduit systems at depth is difficult to observe but can be inferred from the geodynamic history and/or groundwater's isotope data indicating recent hypogene activity (see *Isotopes in groundwater indicating hypogene origin* section).

### The neotectonic period

By the end of the Oligocene, most of the terranes of the Anatolian Peninsula, except a narrow seaway between the Arabian Platform and the Anatolide-Tauride tectonic unit in southeastern Anatolia, were united into a single landmass. Later on, the Miocene collision between the Arabian Platform and Anatolide-Tauride tectonic plates removed the last remnants of the Neotethys Ocean in Anatolia.

The neo-tectonic epoch in Turkey, marked by widespread calc-alkaline magmatism and continental sedimentation, is related to this most recent collision (e.g., Okay, 2008; Göncüoğlu, 2010). The magmatism has become intraplate alkaline since the late Miocene. This change seems to be associated with the flow of the asthenospheric mantle beneath Anatolia. The extension and strike-slip faulting that resulted from the Hellenic Trench's southward migration and the Aegean Sea's emergence as a back-arc basin dominated the new tectonic regime during the Neogene-Quaternary.

The regional uplift of Anatolia was initiated in the east and propagated westward. Oceanic crust subduction, followed by mantle upwelling under Anatolia in the post-Middle Eocene period, maintained the region above the sea. The late Miocene rupture of the subducting oceanic slab in the Eastern Mediterranean Sea induced the uplift of the Tauride (Okay et al., 2020). The Tauride underwent an uplift of 0.2–0.4 km/Myr (Cosentino et al., 2012; Schildgen et al., 2014) after rising above sea level in the late Miocene (8 Myr). The uplift rate increased to over 1 km/Myr in the last 0.6 Myr (Öğretmen et al., 2018). This indicates that the spatio-temporal pattern of uplift in Anatolia cannot be explained merely by the geometry of active deformation, crustal thickness variations, or flexural processes. Recent research indicates that the basaltic magmatism that occurred over the last 10 Myr requires the melting of an anomalously hot asthenospheric mantle beneath the Anatolian Plateau (McNab et al., 2018). Turkey does not have an active volcano today, but the Global Volcanism Program currently lists 10 volcanic systems in Turkey with activity in the Holocene, and additional three volcanoes have historically recorded eruptions (GVP, 2013).

The geodynamic history of the Tauride Karst Belt outlined above shows that proper conditions of hypogene karst development, including the existence of geodynamic fluids, thermobaric and compaction expulsion, metamorphism, high hydrostatic and lithostatic pressures, porosity and hydraulic conductivity development due to hydrofracturing, etc., existed almost throughout the entire Alpidic orogeny.

### HYPOGENE KARST DEVELOPMENT IN THE TAURIDE KARST BELT

A common feature in all of the hypogene karst examples is the greatness of dissolution spaces, deposited rock mass, and mineralization zones. These exceptional sizes are associated with the enormous amount of carbon dioxide and heat released from hypogene processes like magmatism and metamorphism.

#### Carbonate-hosted ore deposits

Iron and lead-zinc ores are the main types of carbonate-hosted mineralization developed by the combination of hypogene and epigenetic processes throughout the Tauride (Fig. 3). In some places, lead-zinc and iron ores are located very closely to each other.

During the late Neoproterozoic, an arc magmatism was developed on the continental margin of Gondwana Land as a result of southeastward subduction of the Proto-Tethys Ocean beneath the Tauride-Anatolide Platform. The volcanic arc was widened by the continuing collision and decreasing subduction angle. Later on, rifting occurred in the back-arc basin in the early Cambrian. Meanwhile, submarine volcanics of mafic or intermediate composition were erupted and deposited contemporaneously with flysch-type sediments, resulting in a volcano-sedimentary series. In this tectonic environment, the formation waters with appropriate pH and Eh values lead to the precipitation of stratiform and stratabound iron and lead-zinc minerals (e.g., Haniççi & Öztürk, 2011; Haniççi et al., 2019).

Following the primary mineralization, formations are affected by post-depositional deformation and metamorphic processes, and uplifted by tectonic forces. Sometime after the Oligocene, when Anatolia became a continental landmass, the cover on the primary ore-bearing formations eroded to the degree that the oxygen-rich, deep-circulating hydrothermal meteoric waters remobilized primary sulfidic ore minerals. The fault zones paved the way for the karstification of overlying carbonate formations by the ascending acidic waters rich in metal ions. The mixing of ascending hydrothermal water with the shallow-circulating oxygen-rich groundwater resulted in the formation of secondary metal carbonate, oxide, and oxy-hydroxide minerals of stratiform and stratabound types. Fluid inclusion studies conducted in carbonate-hosted ore minerals, revealed low formation temperatures (~110-210°C, e.g., Haniççi et al., 2019), suggesting that a secondary ore-forming process occurred in a near-surface environment where ascending metal-rich hydrothermal hypogene fluids

were mixed with oxygen-rich epigenetic groundwaters.

The primary iron ores in the Eastern Taurides formed in late Neoproterozoic (635-541 Myr) - early Cambrian (541-521 Myr) sedimentary rocks. Main iron minerals, from bottom to top, are pyrite (FeS<sub>2</sub>), siderite (FeCO<sub>3</sub>), and hematite (Fe<sub>2</sub>O<sub>3</sub>). The primary sedimentary (stratiform) iron minerals were mobilized by hydrothermal fluids through the fracture zones and redeposited as secondary (stratabound) iron minerals (e.g., siderite and hematite) in veins in the overlying metacarbonates. Hematite is the main mineral in secondary, carbonate-hosted iron deposits in the Tauride.

Like iron deposits, numerous carbonate-hosted Pb-Zn deposits are observed in the Taurides. Similar to the secondary iron ore deposits, the primary sulfidic ores were almost completely replaced with karstic-infill type high-grade Zn-Pb oxide, and carbonate deposits. They occur in Middle Devonian dolomites and dolomitic limestones, Upper Permian and Lower-Middle Triassic allochthonous units (e.g., Aladağlar Unit), and in Jurassic limestone and dolomitic limestone of the autochthonous Geyik Dağı Unit. Mineralizations are stratabound, vein, and karst-infill types and are usually deposited along zones with karstic cavities. Some deposits filling karstic cavities have lenticular shapes with dimensions reaching 50 × 50 × 5 m (width, length, and thickness). The Aladağlar Mountains, comprising the Aladağlar tecto-genetic unit, host many secondary Pb-Zn deposits in the Lower-Middle Triassic limestone-dolomite formation in which the Kuzgun Cave developed (Klimchouk et al., 2006b; Törk, 2008). Kuzgun, with its 1,400 m depth, is the 19th deepest cave in the world as of 2024. It is mainly an epigenetic dissolution system developed almost vertically but also includes hydrothermal chambers in its upper section. In Kuzgun Cave, the epigenetic shafts cut through meter-sized, empty silicate nodules, which can accommodate a person, and which are the remnants of the hypogene karst development period. Groundwater's dissolved helium isotope content reveals a continuing hypogene gas flux in the Aladağlar karst aquifer (see *Isotopes in groundwater indicating hypogene origin* section).

The mineral assemblages of ore bodies include sphalerite (Zn,Fe)S, galena (PbS), pyrite, marcasite (FeS<sub>2</sub>), rare chalcopyrite (CuFeS<sub>2</sub>), arsenopyrite (FeAsS) as primary sulfides; and anglesite (PbSO<sub>4</sub>), cerussite (PbCO<sub>3</sub>), smithsonite (ZnCO<sub>3</sub>), hydrozincite Zn<sub>5</sub>(CO<sub>3</sub>)<sub>2</sub>(OH)<sub>6</sub>, zincite (ZnO), siderite, and hematite as their oxidation products. Fluorite (CaF<sub>2</sub>) and barite (BaSO<sub>4</sub>) are secondary minerals, and quartz (SiO<sub>2</sub>), calcite (CaCO<sub>3</sub>), and dolomite (CaMg(CO<sub>3</sub>)<sub>2</sub>) are the gangue minerals. Alteration is represented by silicification and dolomitization. Fluid inclusion analyses of barite, quartz, and sphalerite revealed formation temperatures ranging from 70 to 160°C. The oxygen and deuterium isotope compositions indicate a meteoric origin for the fluids. According to the common genetic model, the carbonate hosted secondary Pb-Zn deposits in the Taurus Mountains Range, formed by the circulation of deep meteoric waters that mobilized the primary Pb and Zn metals from the basement rocks, and Ba from the marine sediments. The isotope

data indicate that Pb and sulfur in galena were derived from an upper continental crust source, and Ba in barite from a sulfate-rich evaporitic reservoir.

The pH-Eh (oxidation-reduction, redox potential) diagrams can be used to understand the conditions leading to the formation of primary and secondary metallic ore deposits. Figure 5 is a typical diagram that shows the stability fields of various iron minerals and ions according to the pH and oxidation-reduction potential (Eh) conditions of the solution. The exact boundaries between the species shown in the figure vary depending on factors like the activity of the species and the solution composition. However, the figure can still be used to assess the geochemical conditions. Positive Eh values indicate oxygen-rich, oxic or oxidative environments, whereas oxygen-poor or oxygen-depleted, anoxic, or reductive conditions are indicated by negative Eh values. The pH of meteoric waters in local and intermediate depths varies between 6.5 and 8.5. Deep hydrothermal and juvenile/magmatic waters are more acidic due to crustal hydrogen flux and proton-producing redox reactions. Furthermore, high pH waters, dissolving ultramafic rocks, are observed at local and intermediate depths.

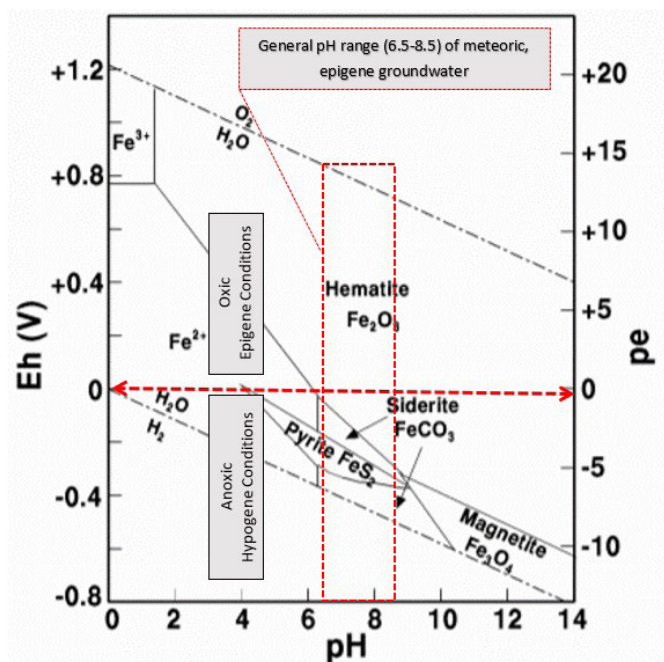


Fig. 5: A typical Eh-pH diagram showing the stability fields of various iron minerals and ions.

Throughout the Tauride, the main primary and secondary iron minerals are pyrite with siderite and hematite, respectively. Figure 5 shows that, within the pH range mentioned above, pyrite and siderite are formed under anoxic conditions, and the precipitation of secondary iron ores like hematite requires dissolved oxygen. Moreover, weathering of pyrite by dissolved oxygen produces sulfuric acid ( $H_2SO_4$ ), which in turn dissolves overlying metacarbonates, in which hematite is precipitated as a secondary iron mineral. Protons (i.e.,  $H^+$ ) produced during the formation of hematite cause additional dissolution of carbonate minerals. The source of oxygen required in the above reactions is the groundwater at shallow to intermediate (i.e., epigene) circulation depths. The hypogene groundwater of deep

circulation and the hydrothermal seawater are anoxic due to dissolved oxygen consumption by organic matter and mineral oxidation. Hence, the oxic and anoxic conditions can be regarded to some extent as characteristic geochemical mediums of epigene and hypogene fluids, respectively.

### Kırkgöz underwater cave system and the Antalya Travertine Plateau

The Kırkgöz underwater cave system and the Antalya Travertine Plateau are outstanding examples of hypogene karst development in the Tauride. Antalya Travertine Plateau, located in the Western Tauride, is the largest freshwater travertine deposit in the world. The travertine has been deposited by the Kırkgöz Springs, behind which the Kırkgöz underwater cave system extends within the Geyik Dağı Unit. The Kırkgöz Springs are located at the northwestern end of the travertine plateau (Fig. 6).

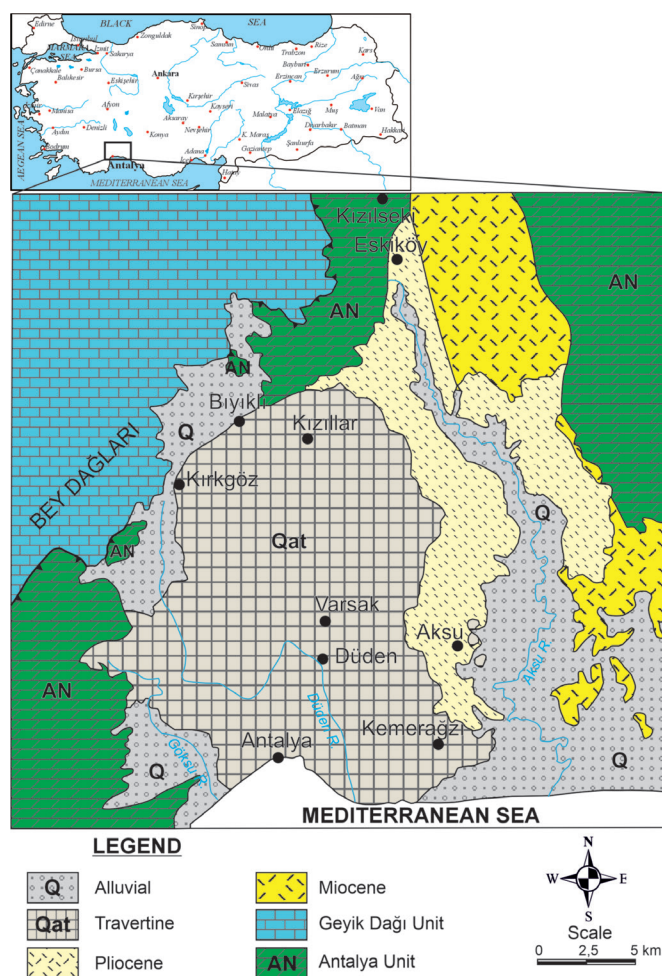


Fig. 6. Geological map of the Antalya Travertine Plateau (modified after Koşun et al., 2019).

### Kırkgöz Springs and underwater cave system

The Kırkgöz Springs (forty outlets) are a group of karst springs emerging from a number of caves and pools. Along with the Düden Spring ( $\sim Q = 10.0 \text{ m}^3/\text{sec}$ ) located in the center of the plateau, the Kırkgöz ( $\sim Q = 18.5 \text{ m}^3/\text{sec}$ ) Springs are the main sources of groundwater that sustain the current travertine formation. A team of US and Turkish cave divers explored the submerged part of these springs in 1995 and discovered a very large and deep underwater cave system. One of the submerged cavities in the Kırkgöz

underwater cave system was named "Stadium" based on its huge dimensions of  $>100 \times 60 \times 50$  m. The Stadium was considered to be the largest submerged cavity in the Asian continent (Kincaid, 1999). None of the karst springs in the Tauride host submerged cavities that are comparable to the Stadium and have formed such a large travertine deposit. The immense amount of dissolution just behind the springs and the voluminous travertine formation deposited by the springs require an enormous amount of aggressiveness, which could be supplied only by hypogene sources.

The diver team also discovered the main submerged feeder conduit of Düden spring, which extends 65 m down below the water surface for about 400 m. Kırkgöz and Düden submerged cave explorations were terminated due to the technical limitations of SCUBA diving (Fig. 7). The volume of the mappable Kırkgöz underwater cave system was calculated as  $410,700 \text{ m}^3$  which can be compared to the underwater conduit network of Wakulla Spring ( $650,000 \text{ m}^3$ ) in Florida, USA, the largest and deepest freshwater spring in the world (Kincaid, 2000).

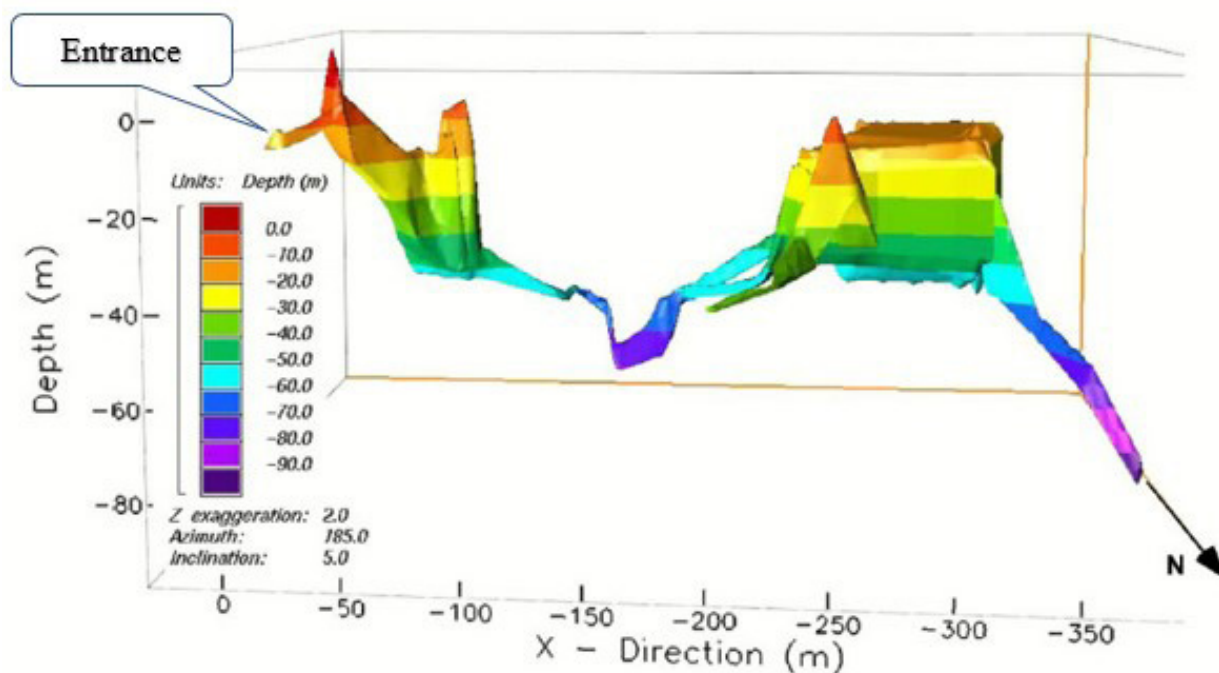


Fig. 7. 3D volumetric model of the Kırkgöz underwater cave system (Kincaid, 1999, 2000).

The saturated volume of the aquifer feeding the Kırkgöz Springs was estimated at 71 billion  $\text{m}^3$  by means of lumped-parameter (LP) modeling of the groundwater's tritium content available for the 1963-2000 period (Özyurt, 2007). The models revealed extraordinary long groundwater mean residence times (MRT) ranging between 103 and 137 years, and the most likely MRT was 120 years. A MRT value of 103 years was also estimated by the tritium/tritiogenic helium method (Özyurt et al., 2000). The presence of a large and deep-circulating groundwater system behind the Kırkgöz Springs is also indicated by the low  $^{14}\text{C}$  activities of the groundwater, which range between 12.1 and 22.4 pmc (Nativ et al., 1999).

Unsurprisingly, the saturated volume of the karst aquifer feeding the Kırkgöz Springs estimated by the LP modeling of groundwater's temporal tritium content is comparable to the volume of the travertine deposited in the Antalya Travertine Plateau. UNDP (1983) estimated the volume of travertine mass deposited by Kırkgöz Springs as 50–60 billion  $\text{m}^3$ .

The presence of such a large freshwater travertine deposit and associated karst springs with huge feeder conduit systems are apparently linked with hypogene fluid migration through the large Geyik Dağı carbonate massif of the Taurus Mountains. In this part of the Eastern Mediterranean, the Rhodes Basin ( $-4,500$  m),

Finike Trough ( $-3000$  m), and Antalya Basin ( $-2,500$  m) mark the extent of a suture zone between the Anatolide-Tauride tectonic unit and the subducted plate of the southern branch of the Neotethys Ocean. Earthquakes with epicenter depths up to 150 km below the surface indicate a continuing and relatively rapid subduction of an oceanic crust along the suture zone. Such deep tectonic activities are also evidenced by the dissolved noble gas data obtained from the karst springs in the Antalya Travertine Plateau, as explained below (Özyurt et al., 2000).

#### Antalya Travertine Plateau

The Antalya Travertine Plateau (Fig. 8) extends as three continuous and step-wise plateaus covering an area of  $630 \text{ km}^2$ . Its maximum thickness is about 280 m. Antalya travertine is bounded by Antalya and Geyik Dağı tectono-stratigraphic units from the west and north and by the Mediterranean Sea from the south. At the east, it unconformably overlies the Pliocene conglomerate and is bounded by Quaternary fluvial sediments. The extent of travertine deposits in the west-east and north-south directions is around 19–30 km and 29–34 km, respectively (Koşun et al., 2019).

Antalya travertine is divided into "upper", "middle", and "lower" plateaus, all of which are almost flat, with a gentle slope toward the Mediterranean Sea. The

plateaus are separated by cliffs extending roughly in a west-east direction. The heights of the cliffs separating the upper-middle and middle-lower plateaus range

between 40-60 m and 10-40 m, respectively. The cliffs formed due to rapid uplift and/or sea level changes during the Quaternary.



Fig.8. Aerial view of the Antalya Travertine Plateau with Düden River cascading into the Mediterranean Sea (looking northwest).

The upper plateau (Döşemealtı Plateau) extends between 200-320 m (a.s.l.) and has a thickness between 280 and 100 m, thinning westward. The middle plateau (Düden or Varsak Plateau), with a thickness ranging between 65 and 85 m, is tilted toward the Mediterranean Sea between 180 and 40 m (a.s.l.) elevations. The lower plateau (submarine) starts from about the present sea level, extends down to -50 to -100 m below sea surface, and terminates with a 50 m-high underwater cliff at about 2.5 km offshore (Koşun et al., 2019). The areal extent of the submarine travertine plateau is estimated from the sea floor topography to be around 25 km<sup>2</sup>.

According to Glover & Robertson (2003), Antalya Travertines were deposited from cool karstic spring waters in a N-S-trending half-graben bordered by the Taurus Mountains from the west. The lacustrine/paludal travertine deposition started in the late Pliocene, following the regression of a shallow sea. The deposition occurred in and around numerous small lakes bounded by NS trending extensional fault blocks. The deposit has complex facies associations, including shallow lakes, marshes, and sluggish streams.

According to an unpublished document, the age of travertine is also defined as late Pliocene based on Ostracoda fossils found in a drilling in the sands encountered at the bottom of the travertine. Some of the <sup>230</sup>Th/<sup>234</sup>U ages obtained from travertines are >600 kyr, which is the upper limit of this dating method (Glover & Robertson, 2003). The late Pliocene can be accepted as the time of the initiation of groundwater discharge from the Kırkgöz springs.

Glover & Robertson (2003) conclude that the climatically favorable time for maximum travertine deposition was the early-mid Pleistocene (2.0-1.5 Myr). In this period, the climate was cool but seasonally stable, so the discharge of the Proto-Kırkgöz Springs was never interrupted. Basin wide, large-scale, and extensive travertine deposition is thought to have restricted or ended when the lakes and marshes shrank during the mid-late Quaternary glacial climate

periods (e.g., Çiner et al., 2015; Çiner & Sarıkaya 2017). The Quaternary glaciations that occurred in the high mountain sector that serves as the recharge area of Kırkgöz Springs caused the precipitation in the mountain sector to remain partly blocked during the ice phase, so that the groundwater recharge was reduced substantially during these periods. Hence, during the glacial periods of the Quaternary, the discharge of the Kırkgöz springs and associated travertine deposition should have slowed down, if not stopped. In other words, the Quaternary glaciations not only scraped epigene karst morphology in the high mountains but also slowed down the hypogene karst development by reducing the amount of groundwater in deep circulation, whereas the carbon-dioxide input from hypogene sources was continuous.

The continuing gradual tectonic uplift and the glacio-eustatic sea-level fluctuations during the Middle Quaternary favored localized stream erosion and created the irregular cliffs and promontories of the second main terrace along the paleo-coastline. Currently, relatively small volumes of spring water continue to flow at different levels of the terrace system and deposit travertine along stream beds, waterfalls, and cascades.

The formation of a cliff between the upper and middle plateaus seems linked to a rapid uplift event. Ögretmen et al. (2018) point out a rapid uplift event at early Middle Pleistocene (ca. 475 kyr) based on the fact that the fossil records of a benthic marine fauna that was associated with the paleo-coastline are now located at 1,500 to 1,600 m a.s.l. They conclude that, such a fast uplift (~3 mm/yr) of the southern margin of the Central Anatolian Plateau (i.e., Taurus Mountains) after the early Middle Pleistocene can be linked to lithosphere delamination and subsequent slab breakoff (i.e., the Antalya Slab; Güvercin et al., 2021) during the continental collision of the Arabian and Anatolian Plates. This tectonic activity seems to have triggered a young volcanic activity phase in the Central Anatolian part of the Tauride tectonic unit,

which lead to the formation of the obruks, the giant dolines of hypogene karst (see following chapter).

The third travertine plateau was formed around the Last Glacial Maximum (~20 kyr ago) when the global sea level lowered about 130 m with respect to the current level. The sculpting of present-day coastal cliffs started after the post-glacial sea level rise at about 10 kyr.

### Obruks - giant dolines of hypogene karst development

Obruk is a Turkish geomorphic term (UNESCO, 1972), describing mega-collapse dolines with surface diameters and depths reaching several hundreds of meters (Fig. 9). They are commonly formed in the Konya Closed Basin (KCB), which is a part of the Anatolide-Tauride tectonic unit. A detailed assessment of the formation of obruks is presented in Bayarı et al. (2009a, 2017).



Fig. 9. Kızören Obruğu is the largest (350 m wide and 225 m deep) obruk in the KCB. In the front is a medieval-age caravanserai. The lake is the exposed groundwater table.

The obruks developed mostly in the Neogene lacustrine limestone, which is overlain in many places by the Plio-Quaternary lacustrine clastics. Therefore, the initiation of the formation of the oldest obruks can be constrained in the early Pliocene. Currently, new obruks continue to form with an annual frequency, but they have a much smaller size. Their formation is associated with the cover collapse of large saturated dissolution cavities in the Neogene limestone as a result of the reduced buoyancy force of the groundwater as it is lowered by intensive regional abstraction for irrigation.

Processes leading to obruk formation have long been a matter of debate. Proposed formation mechanisms

include volcanic explosion as in the case of maar formation (e.g., Frech, 1916 in Erinç, 2001), enhanced dissolution caused by highstands of the pluvial lakes during the wet periods of the Pleistocene (Erol, 1986), locally enhanced subsurface dissolution driven by volcanogenic gas discharges (e.g., Canik & Çörekcioglu, 1986), and a combination of hypogene karstification and mixing corrosion between surface recharge and groundwater (e.g., Pekkan, 2004). Recent studies revealed that the formation of obruks is associated with an enormous amount of localized ascending hypogene fluids during the Plio-quaternary magmatism (e.g., Bayarı et al., 2016, 2017, Özyurt & Bayarı, 2018).

The northerly subduction of the African Plate beneath the Anatolide-Tauride tectonic unit from the late Eocene to the early Miocene (40-20 Myr) resulted in widespread contraction and volcanic quiescence (Schleiffarth et al., 2016). The volcanism in the Central Anatolian Volcanic Province (CAVP) was initiated in the final phase of this contraction at around 20 Myr. Phase 1 of volcanism (20-12 Myr) is caused by initial slab foundering and rollback and is characterized by voluminous, mafic-intermediate volcanic centers concentrated mainly in eastern Central Anatolia. Phase 2 slab rollback volcanism continued into the late Miocene (11-5 Myr) and is characterized by an ignimbrite flare-up and eruptions at small, intermediate, polygenetic volcanic centers. They are concentrated in the western CAVP. This volcanic activity terminated with the final closure of the Neotethys ocean in western Anatolia. Phase 3 (4-0 Myr) is the Pliocene to Holocene volcanism, characterized by monogenetic and large stratovolcanoes, and represents the combined effects of slab breakoff and tectonic escape. The volcanic centers are concentrated along young transtensional fault systems, which seem to coincide with the suture zone between the Central Anatolian Crystalline Complex and the Taurides.

The KCB is an endorheic basin where the groundwater flows from the Taurus Mountains (the main recharge area) at the south toward the Salt Lake (the discharge area) at the north (Fig. 10). The radiocarbon age of the groundwater increases from recent at the mountain flank to about 45 kyr at the south of the Salt Lake (Bayarı et al., 2009b). Apart from formation of obruks as giant dissolution structures, a wide range of evidences of hypogenic fluid contributions along the regional flow path include: (i) increasing concentrations of volcanogenic elements like, chloride, fluoride, and lithium, (ii) increasing dissolved  $\text{CO}_2$  (i.e.,  $\log P_{\text{CO}_2}$ ) from an air-water equilibrium value of  $-2.2$  atm at the foot of Taurus Mountains to about  $-1.0$  atm in the rest of the regional groundwater flow path, (iii) enriched  $\delta^{13}\text{C}$  signals typical of  $\text{CO}_2$  originating from mantle and crustal sources, (iv) flowing artesian groundwater discharges rising 10-30 m from ground surface with abundant dissolved  $\text{CO}_2$  (>95%) having  $^{13}\text{C}$  contents of around 0 ‰, (v) high dissolved He contents with elevated R/Ra values which are indicative of crustal and mantle gas input and (vi) young volcanism with  $^{40}\text{Ar}/^{39}\text{Ar}$  ages ranging between 0.096 and 9.2 kyr before present.

It is apparent that the formation of giant obruks is a consequence of the hypogene karst development evolved with a complex interaction among the geological, geochemical, and hydrogeological factors,

which are governed by the geodynamic evolution of the Taurides. Figure 11 shows the outlines of a conceptual model of hypogene processes inferred to be occurring during this evolution.

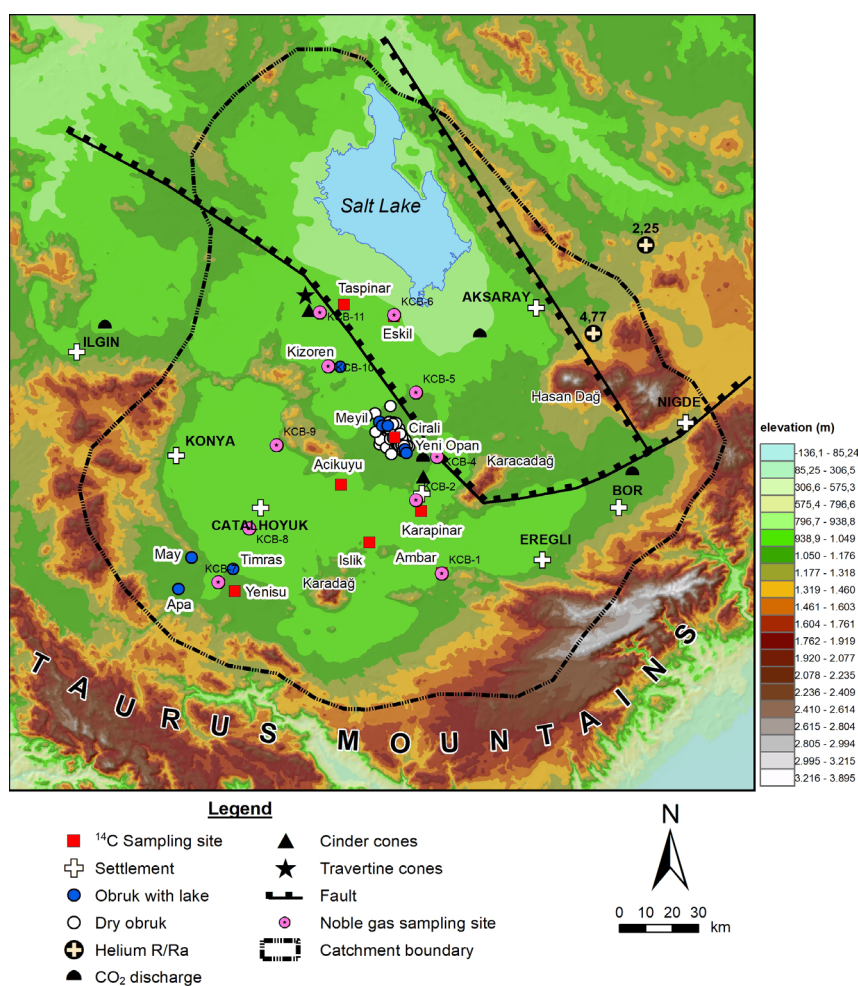


Fig. 10. Morphological map of the KCB, showing obruks and associated features (modified after Bayari et al., 2017).

The main driver of the hypogene karst development in the KCB is the geogenic carbon-dioxide flux supplied from the upper continental crust and mantle as a result of the magmatism and metamorphism occurring since the late Miocene. The extensional tectonics, which is present particularly after the Pliocene, resulted in a lithospheric thinning and accompanying asthenospheric rise under the KCB. The concurrent volcanism, which is currently in a dormant phase, continued episodically almost until today. It is likely that an accountable portion of the carbon-dioxide has been produced by metamorphism (e.g.,  $\text{CaCO}_3 + \text{SiO}_2 + \text{heat} = \text{CaSiO}_3 + \text{CO}_2$ ), which is driven by the mantle and crustal (i.e., radiogenic) heat flux.

According to the conceptual model in Figure 11, the fresh epigene groundwater moving from the Taurus Mountains toward the Salt Lake is mixed with ascending hypogene thermal groundwater seeping into the superficial aquifer. The upward migration of hydrothermal fluid is driven by the density gradient created by crustal and mantle heat flux as well as episodic seismic and volcanic activities. The carbon dioxide dissolved in the ascending hydrothermal fluid starts to degas as the hydrostatic pressure acting upon it decreases toward the surface. Eventually, the increasing release of gas bubbles and the decreasing

hydrostatic pressure acting upon them result in a larger gas-liquid interface and more carbonic acid production. This process enhances the dissolution in near-surface environments like the base of obruks, which seem aligned with fault zones acting as tectonic pathways of  $\text{CO}_2$ -rich groundwater migration. Hydrothermal convection cells are formed along these pathways as the groundwater cools in a near-surface environment due to the heat flux toward the atmosphere. Almost all of the morphologically old-looking obruks have a larger size compared to recent formations and are located in the Obruk Plateau, in the unconfined part of the regional groundwater flow path (Fig. 10).

The old obruks developed along a northwest-trending quasi-linear zone, which seems to coincide with a fault zone extending along an intrasuture of the Anatolide-Tauride tectonic unit. On the other hand, young obruks are aligned with a northeast trending zone that is parallel to the line of Karadağ, Karacacadağ, and Hasandağ young volcanoes (Fig. 10). Hence, the formation of recent obruks seems to be associated with Phase 3 volcanism, which has been active since the last 4 Myr. The  $^{40}\text{Ar}/^{39}\text{Ar}$  ages of the youngest volcanism ranges between 0.096 and 9.2 kyr before present.

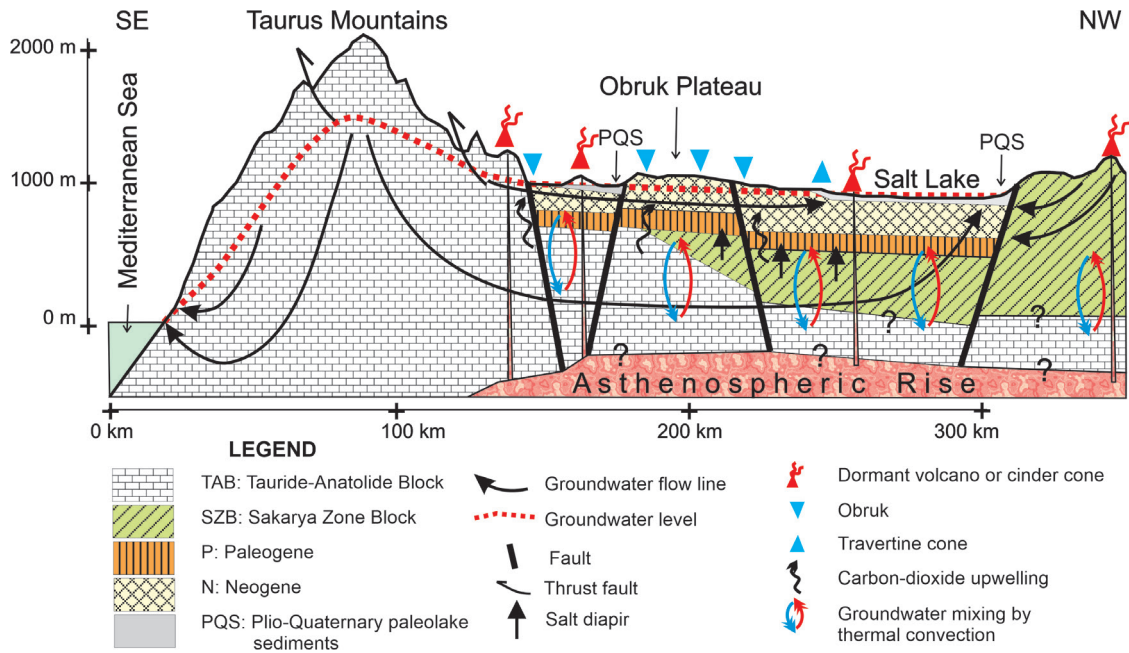


Fig. 11. Conceptual model of the hypogene karst development in the central part of the Tauride tectonic unit (modified after Bayarı et al., 2017).

### Isotopes in groundwater indicating hypogene origin

Isotopic signals contained in dissolved solids and gas species in groundwater provide decisive evidence of hypogene processes that may not be observed directly at the surface. The helium isotope ratios and the  $^{13}\text{C}$  isotope content of the groundwater discharging from the huge submerged cavities behind Kırkgöz Springs and from other springs of the Antalya Travertine Plateau (west of Central Tauride), from the springs of Aladağlar Massif (east Central Tauride), and through the superficial Neogene aquifer of the KCB revealed apparent evidence of hypogene fluid input from the crustal and mantle sources.

Helium isotopes have characteristic signals from end-member sources like the atmosphere, crust, and mantle. Helium has two isotopes: helium-3 ( $\text{He-3}$ ) and helium-4 ( $\text{He-4}$ ). Other isotopes of helium have lifetimes of less than a second. Sources of  $\text{He-3}$  in groundwater are the atmosphere, fission of  $\text{Li-6}$ , which is a product of  $\text{U-Th}$  decay in the crust, escape from the mantle, and the decay of tritium isotopes in water molecules. Sources of  $\text{He-4}$  in groundwater are the atmosphere and  $\text{U-Th}$  series decay in the crust. The mantle source of  $\text{He-4}$  is negligible.

The helium isotope ratio is presented by the "R" notation ( $R = \text{He-3}/\text{He-4}$ ). The atmospheric  $\text{He-3}/\text{He-4}$  ratio ( $R_a$ ) is  $1.38 \times 10^{-6}$ . Because of the continuous mixing of the atmosphere, this number is spatio-temporally fixed. Measured helium gas ratios ( $R$ ) are generally shown as  $R/R_a$  and the typical  $R/R_a$  values of the atmosphere, crust, and mantle end-members are 1, 0.05, and 8, respectively (e.g., Ozima & Podosek, 1983).

The  $R/R_a$  values measured in Kırkgöz and Düden springs in the Antalya Travertine Plateau vary between 2.60 and 1.47 (Nativ et al., 1999). The  $R/R_a$  value of 2.60 is the highest ratio measured in the cool karst springs in Turkey. This high  $R/R_a$  ratio apparently indicates a heat and mass flux from the mantle and

the upper continental crust beneath the Kırkgöz karst aquifer. The low  $^{14}\text{C}$  activity (12.0 - 22.4 pmc), exceptionally high He content (429-991  $\mu\text{cc}/\text{kg}$ ) and  $R/R_a$  ratios (1.47-2.60), high carbon-dioxide content (up to 83 mg/L) and enriched  $\delta^{13}\text{C}$  values (-2.2 to -4.1‰) measured by Nativ et al. (1999) in Kırkgözler and other karst springs in the Antalya Travertine Plateau are other indicators of hypogene fluid contribution from the crust and mantle. Enriched  $\delta^{13}\text{C}$  values (around 0‰) have also been observed in the groundwater in the superficial Neogene aquifer of the KCB.

Figure 12 shows the scatter plot of  $\text{He-3}/\text{He-4}$  versus  $\text{Ne}/\text{He}$  ratios of the groundwater samples collected from Kırkgöz and Düden Springs (KKA), springs of Aladağlar Massif (AKA), and from the superficial Neogene aquifer in the Konya Closed Basin (KCB) of the Tauride tectonic unit (Özyurt & Bayarı, 2014) (Fig. 1). All samples indicate hypogene gas flux from the crust and mantle, although some of them include an atmospheric contribution, probably because of the contamination during the sampling or due to contribution from epigenic young groundwater.

### Pumping of hypogene fluids by the earth-tides

Earth-tides are known to affect the poroelasticity of rocks and hence the fluid flux rate and direction in cool and hot water springs, (e.g., Rinehart, 1976; Williams, 1977; Martin et al., 2012; Alcérreca-Huerta et al., 2023), cool and hot water aquifers (e.g., Valois et al., 2024; Schultz et al., 1996), and petroleum reservoirs (e.g., Arditty, 1978). Moreover, the upper crust also fluctuates with the seasonal recharge load, as in the case of the Amazon River Basin (e.g., Bevis et al., 2005).

In the near-surface part of the upper continental crust, groundwater is driven mainly by the earth's gravity and external pressures (i.e., lithostatic, tectonic, seismic, etc.). The hydrostatic pressure ( $P_s$ ) is determined by the earth's gravity that is exerted on the fluid mass, whereas the other pressures exerted

on the medium from outside cause an excess pressure ( $P_{ex}$ ) for pore water. This influences the transport of groundwater in aquitards. The earth tides are generated by the total tide generating force (TGF) of

the horizontal components of the sun and moon. On the other hand, the atmospheric precipitation falling on the ground creates a recharge load (RL) on the aquifer. This force acts on the pores vertically.

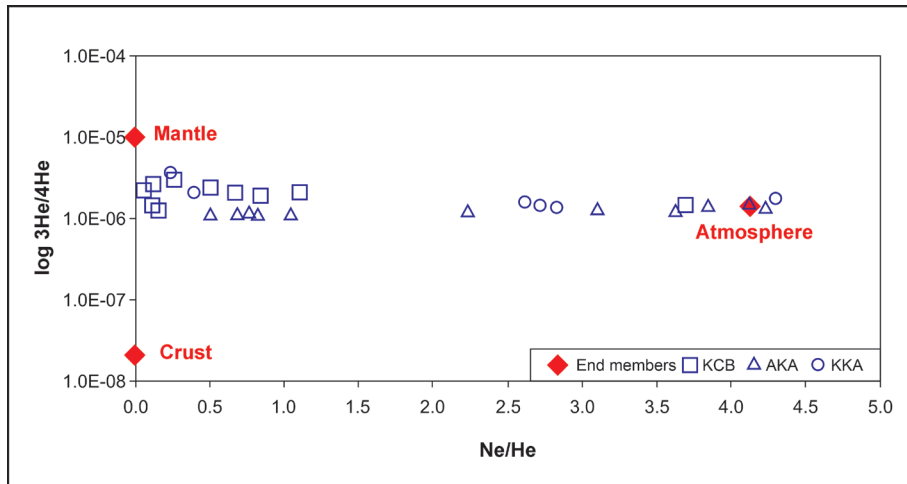


Fig. 12. He-3/He-4 vs Ne/He ratios of the groundwater samples collected from the various karst aquifers in the Taurides (after Özyurt & Bayari, 2014).

High temporal-resolution seawater specific electrical conductivity and temperature observations conducted in the Mivini submarine cave revealed periodic oscillations of the freshwater discharge rate (Bayari & Özyurt, 2014). The cave, discharging groundwater from the deep karst aquifer of the Geyik Dağı Unit of the Taurides, is located on the southwestern coast of the Taurus Mountains Range (Fig. 1). The recharge area of the aquifer extends between sea level and >3,000 m elevation. The cave developed as a tubular conduit along the seawater-freshwater interface. It starts 4 m below the sea level and extends down to -80 m, which was the divers' technical limit. Temporal

specific electrical conductivity and temperature data were collected by a data logger placed on the ceiling of the cave at -20 m below sea level. The freshwater content supplied by the karst aquifer shows a sinusoidal pattern with an amplitude that varies temporally (Fig. 13). The sea tide range in the Eastern Mediterranean Sea, where the Mivini Cave is located, is in the order of about 20 cm. Therefore, the coastal karst springs along the Taurus Mountains Range do not exhibit salinity fluctuations due to the sea tides. Relative sea level variations observed at Antalya Mareograph Station, located 130 km northeast of the cave, are mainly correlated with changes in air pressure (Fig. 13).

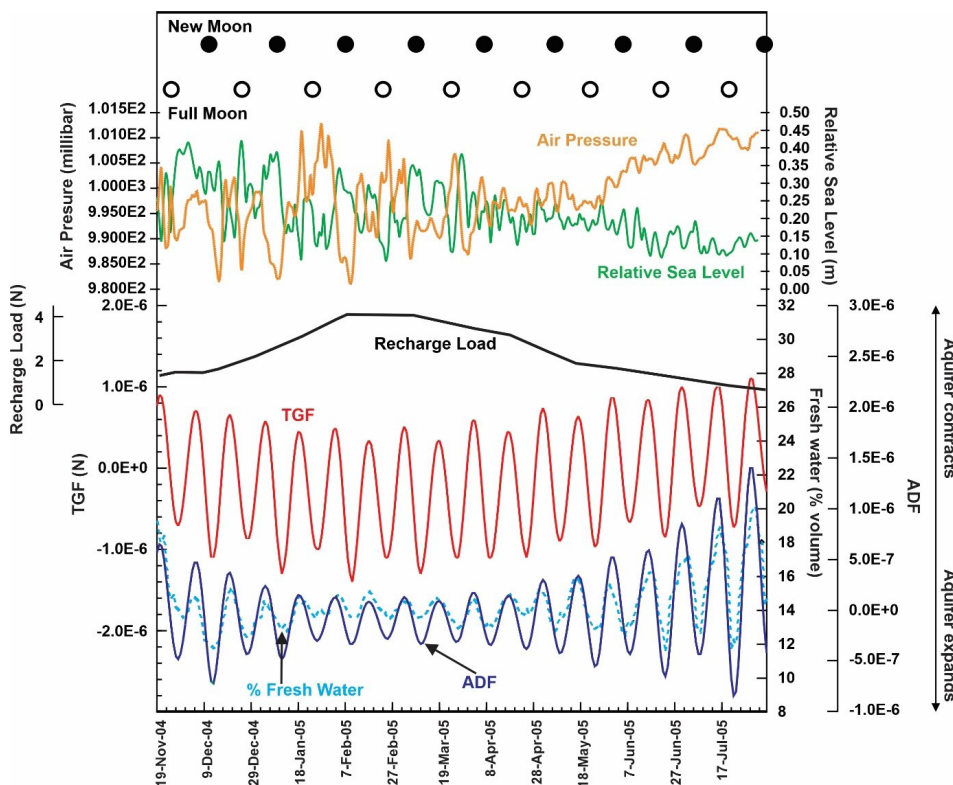


Fig. 13. Temporal variations of % fresh water content of groundwater discharging from Mivini Cave, air pressure, relative sea level, recharge load, tide-generating force (TGF), and aquifer deformation factor (ADF) (modified after Bayari & Özyurt, 2014).

The magnitude of the freshwater content of the groundwater discharging from the cave ranged between 11 and 21% by volume during the observation period. The cycles of increasing and decreasing freshwater content are in phase with the cycles of TGF calculated for this area (Fig. 13). However, the amplitude of cycles of freshwater content and those of TGF are not identical, although their long-term trends are similar. On the other hand, the temporal signal of freshwater content exhibits an almost perfect match to the Aquifer Deformation Factor ( $ADF = TGF/RL$ ). The TGF acts in a horizontal direction, and the increasing and decreasing values of TGF cause compression and expansion of the aquifer, respectively. The magnitude of elastic deformation exerted on the aquifer by TGF is reduced by the RL, which acts in a downward direction. As a consequence, the discharge of the karst aquifer driven by TGF is reduced during the wet season (i.e., the winter of the northern hemisphere) when the elevated RL limits the horizontal poroelastic deformation. Hence, the ADF is an indicator of the overall variation in poroelasticity. Increasing RL inhibits the lateral compression and expansion dictated by TGF, and vice versa. The lower the RL, the more efficient the TGF. Therefore, both the magnitude and the value of ADF determine the freshwater content of the groundwater coming out of the submerged conduits of the aquifer.

Bayarı & Özyurt (2014) developed a numerical model that accounts for the interaction between TGF and RL to calculate the temporal variation of expected poroelasticity, which fits well with the temporal variation of percent fresh water discharging from the cave (Fig. 13). Results of the model reveal that the earth-tide can also be an effective flow driver for hypogene karst development in the deep parts of the upper continental crust where gravity-driven flow is hindered or impossible.

## CONCLUSIONS AND OUTLOOK

The reassessment of the field observations and laboratory data collected during the last two decades provided important evidence on the relation between the evolution of hypogene karst and the geodynamic history of the western and central Taurides. The widely scattered carbonate-hosted secondary ore deposits indicate that a vast hypogene karstification along with metasomatism occurred in the Taurus Mountains Range. The initially hypogene minerals have been converted to secondary ore deposits upon contact with oxygen-rich meteoric water circulating at local to intermediate depths. The magnitude of hypogene dissolutions and associated surface deposits is huge because of the vast amount of magmatogenic and metamorphic carbon dioxide supplied to the karst aquifers. The Kırkgöz submerged cave system and the Antalya Travertine Plateau, which is the world's largest deposit precipitated from cool karst groundwater, are outstanding examples of the scale and consequences of this hypogene karst development. Similarly, the obruks, the giant collapse dolines in central Anatolia, indicate how big the impact of ascending hypogene

fluid flow in the upper continental crust, rich in volcanogenic carbon-dioxide, can be. Groundwater's noble gas and carbon isotope data reveal information about the ongoing hypogene activity in the upper crust, where earth-tidal pumping seems to be a potential flow driver for the groundwater at the depths where the circulation is inhibited or impeded.

This study shows that there is a huge potential for hypogene karst development in parts of the world with current or past geodynamic activity. However, a hydrogeological overview of the geodynamic history is essential for assessing the hypogene processes and their reflections on the land surface.  $^{40}\text{Ar}/^{39}\text{Ar}$  dating of the young volcanism and the screening of groundwater's noble gas and carbon isotope signals in areas with potential karst development can be useful to determine existing but asymptomatic hypogene activity.

## ACKNOWLEDGEMENTS

We thank Drs. Christoph Spötl and Daniel Doctor, and an anonymous referee for their critical comments that helped to improve the manuscript. The final review by Dr. Jo De Waele is also acknowledged gratefully. Numerous people and agencies, from abroad and Turkey, have supported our group's studies on different aspects of karst hydrogeology since the 1990s. The list of their names is too long to be listed here. But one name, Alexander B. Klimchouk, deserves to be mentioned especially. First of all, we should admit that this paper should have his name among the authors. This is because many of the ideas expressed here have evolved during the long discussions made with him on the excursions throughout the Tauride since the 1995 Karst Symposium in Antalya. Following the 2000 Karst Symposium hold in Antalya again, we decided to work on the topic of high-mountain, deep-karst in the Aladağlar Massif of east Central Tauride. Starting in 2001, this hard work lasted eight years with the month-long high-elevation camps. Later on, our collaboration continued with the fieldworks conducted almost every summer. We visited every part of the Tauride karst, from coastal zones to mountain peaks of >3,500 m, and in the Anatolian Plateau. Our journey with him started as colleagues, then we became friends and then brothers. One can rarely encounter such a person in the entire life. No hardship, not even the troubles of his illness, could defeat Alexander's desire to learn new things about karst; he worked hard until the very last moment. We have been lucky to meet you, Alexander. Rest in peace!

**Authorship statement:** CSB, NNÖ designed the research and wrote the paper; NNÖ, LN, KAT, İNG, EP, PA conducted fieldworks and contributed to the writing.

## REFERENCES

Alcérreca-Huerta, J.C., Álvarez-Legorreta, T., Carrillo, L., Flórez-Franco, L.M., Reyes-Mendoza, O.F., Sánchez-Sánchez, J.A., 2023. First insights into an exceptionally

- deep blue hole in the Western Caribbean: The Taam ja'Blue Hole. *Frontiers in Marine Science*, 10, 1141160 <https://doi.org/10.3389/fmars.2023.1141160>
- Arditty, P.C., 1978. The earth tide effects on petroleum reservoirs: preliminary study. Unpublished MS Thesis, Stanford University, 280 p.
- Bayarı, C.S., Pekkan, E., Özyurt, N.N., 2009a. Obruks, as giant collapse dolines caused by hypogenic karstification in central Anatolia, Turkey: analysis of likely formation processes. *Hydrogeology Journal*, 17, 327-345. <https://doi.org/10.1007/s10040-008-0351-9>
- Bayarı, C.S., Özyurt N.N., Kilani, S., 2009b. Radiocarbon age distribution of groundwater in the Konya closed basin, central Anatolia, Turkey. *Hydrogeology Journal*, 17(2), 347-365. <https://doi.org/10.1007/s10040-008-0358-2>
- Bayarı, C.S., Özyurt, N.N., Öztan, M., Baştanlar, Y., Varinlioğlu, G., Koyuncu, H., Ülkenli, H., Hamarat, S., 2011. Submarine and coastal karstic groundwater discharges along the Southwestern Mediterranean coast of Turkey. *Hydrogeology Journal*, 19(2), 399-414. <https://doi.org/10.1007/s10040-010-0677-y>
- Bayarı, C.S., Özyurt, N.N., 2014. Earth tide, a potential driver for hypogenic fluid flow: observations from a submarine cave in SW Turkey. In: Klimchouk A.B., Sasowsky, I., Mylroie, J., Engel, S.A., Engel, A.S. (Eds.), *Selected Papers and Abstracts of the Symposium, Karst Waters Institute Special Publication 18*, Leesburg (VA): Karst Waters Institute, 20-24.
- Bayarı, C.S., Özyurt, N.N., Klimchouk, A.B., Tork, K., Nazik, L., 2016. Evidence of hypogenic karst development in the Taurus mountain range, Turkey. In: Chavez, T., Reehling, P. (Eds.), *Proceedings of DeepKarst 2016: Origins, resources, and management of hypogene karst*, New Mexico: National Cave and Karst Research Institute, 67-71.
- Bayarı, C.S., Özyurt, N.N., Törk, A.K., Avcı, P., Güner, İ.N., Pekkan, E., 2017. Geodynamic control of hypogene karst development in Central Anatolia, Turkey. In: Klimchouk, A.B., Palmer, A.N., De Waele, J., Auler, A.S., Audra, P. (Eds.), *Hypogene karst regions and caves of the world*. Springer, Cham, p. 449-462. [https://doi.org/10.1007/978-3-319-53348-3\\_27](https://doi.org/10.1007/978-3-319-53348-3_27)
- Bevis, M., Alsdorf, D., Kendrick, E., Fortes, L.P., Forsberg, B., Smalley R.Jr., Becker, J., 2005. Seasonal fluctuations in the mass of the Amazon River system and Earth's elastic response. *Geophysical Research Letters*, 32, L16308. <https://doi.org/10.1029/2005GL023491>
- Canik, B., Çörekçiöğlu, İ., 1986. The formation of sinkholes (Obruk) between Karapınar and Kızören-Konya. In: *Proceedings of Symposium on Karst Water Resources*, IAHS Publ no. 161, IAHS, Wallingford, UK, p 193-205.
- Cosentino D., Schildgen, T.F., Cipollari, P., Faranda, C., Gliozzi, E., Hudáčeková, N., Lucifora, S., Strecker, M.R., 2012. Late Miocene surface uplift of the southern margin of the Central Anatolian Plateau, Central Tauride, Turkey. *Geological Society of America Bulletin*, 124, 133-145. <https://doi.org/10.1130/B30466.1>
- Çiner, A., Sarıkaya, M.A., Yıldırım, C., 2015. Late Pleistocene piedmont glaciations in the Eastern Mediterranean; insights from cosmogenic <sup>36</sup>Cl dating of hummocky moraines in Southern Turkey. *Quaternary Science Reviews*, 116, 44-56. <https://doi.org/10.1016/j.quascirev.2015.03.017>
- Çiner, A., Sarıkaya, M.A., 2017. Cosmogenic <sup>36</sup>Cl geochronology of Late Quaternary glaciers on the Bolkar mountains, South Central Turkey. In: Hughes P, Woodward, J. (Eds.), *Quaternary glaciation in the Mediterranean mountains*. Geological Society of London Special Publication, 433, 271-287. <https://doi.org/10.1144/SP433.3>
- Eriñç, S., 2001. *Geomorphology II* (3rd ed.) (in Turkish). Der Publication House, Istanbul.
- Erol, O., 1986. The relationships between the phases of the development of the Konya-Karapınar obruks and the Pleistocene Tuz Golu and Konya pluvial lakes. In: Gunay, G., Johnson, I.E. (Eds.), *Karst water resources Proceedings of the Ankara-Antalya Symposium*, IAHS Publication 161, Wallingford, UK, 207-213.
- Ezhov, Y.A., Lysenin, G.P., 1990. Vertical zonation of karst development. *Izvestija AN SSSR serija geologii*, 4, 108-116 (in Russian).
- Ezhov, Y.A., Lysenin, G.P., Andreychouk, V.N., Dublyansky, V.N., 1992. *Karst in the Earth's crust*. Sibirskoye otdeleniye Instituta geologii, Novosibirsk (in Russian).
- Frech, F., 1916. *Geologie Kleinasiens in Bereich der Bagdadbahn* [Geology of Asia Minor as regards the Baghdad Railway]. *Zeitschrift Deutsch Gesellschaft Geowissenschaft*, 68, 1-326.
- Glover, C., Robertson, A.H., 2003. Origin of tufas (cool-water carbonate) and related plateaus in the Antalya areas, SW Turkey. *Geological Journal*, 38, 1-30 <https://doi.org/10.1002/gj.959>
- Göncüoğlu, M.C., Dirik, K., Kozlu, H., 1997. Pre-Alpine and Alpine Terranes in Turkey: Explanatory notes to the terrane map of Turkey. *Annales Géologique Pays Hellénique*, 37, 515-536.
- Göncüoğlu, M. C., 2010. Introduction to the geology of Turkey: Geodynamic evolution of the Pre-Alpine and Alpine terranes. Monography series no. 5, MTA, Ankara, Turkey, 66 p.
- Göncüoğlu, M.C., 2019. A review of the geology and geodynamic evolution of tectonic terranes in Turkey. In: Pirajno, F., Ünlü, T., Dönmez, C., Şahin M.B. (Eds.), *Mineral Resources of Turkey*, Springer, 19-72. [https://doi.org/10.1007/978-3-030-02950-0\\_2](https://doi.org/10.1007/978-3-030-02950-0_2)
- Güvercin, S.E., Konca, A.Ö., Özbakır, A.D., Ergintav, S., Karabulut, H., 2021. New focal mechanisms reveal fragmentation and active subduction of the Antalya slab in the Eastern Mediterranean. *Tectonophysics*, 805, 1-24. <https://doi.org/10.1016/j.tecto.2021.228792>
- GVP, 2013. Global volcanism program (2013), *Volcanoes of the world*, [https://volcano.si.edu/gvp\\_cite.cfm](https://volcano.si.edu/gvp_cite.cfm) [accessed: February 27, 2024].
- Haniñçi N, Öztürk H., 2011. Geochemical/isotopic evolution of Pb-Zn deposits in the Central and Eastern Taurides, Turkey. *Int. Geol. Rev.*, 53(13), 1478-1507 <https://doi.org/10.1080/00206811003680008>
- Haniñçi, N., Öztürk, H., Kasapçı, C., 2019. Carbonate-hosted Pb-Zn deposits of Turkey. In: Pirajno, F., Ünlü, T., Dönmez, C., Şahin M.B. (Eds.), *Mineral Resources of Turkey*. Springer, Cham, p. 497-533. [https://doi.org/10.1007/978-3-030-02950-0\\_10](https://doi.org/10.1007/978-3-030-02950-0_10)
- Hozathoğlu, D., Bozkaya, Ö., Yalçın, H., Yılmaz, H., 2020. Mineralogical characteristics of metamorphic massif units outcropping in Göksun, Afşin and Ekinözü (Kahramanmaraş) region. *Bulletin of the Mineral Research and Exploration*, 162, 105-146.
- Ignatovich, N.K., 1950. Zoning, formation and activity of groundwater in relation with geostructures development. In: *Voprosy gidrogeologii i inzhenernoy geologii* [Questions of hydrogeology and engineering geology] Volume 13, Izdatelstvo MGU, Moscow, 6-22 (in Russian).
- Juteau, T., 1980. Ophiolites of Turkey. *Ophioliti*, 2, 199-238.

- Kincaid, T., 1999. Morphologic and fractal characterization of saturated karstic caves. Unpublished Ph.D. Thesis, University of Wyoming, Laramie, 174 p.
- Kincaid, T., 2000. A method for producing 3-D geometric and parameter models of saturated cave systems with a discussion of applications. In: Sasowsky, I., Wicks, C. (Eds.), *Groundwater flow and contaminant transport in carbonate aquifers*. Balkema, p. 169-190.
- Klimchouk, A.B., Kasjan, Yu., Samokhin, G., Nazik, L., Bayarı, S., Tork, K., Ozel, E., 2006. Kuzgun Cave in the Aladaglar massif, Turkey: recent developments and the perspectives. Abstracts, 2nd Middle-East Speleology Symposium, Lebanon, 52-53.
- Klimchouk, A.B., 2007. Hypogene Speleogenesis: Hydrogeological and morphogenetic perspective. National Cave and Karst Research Institute, Special Paper No. 1, Carlsbad, New Mexico, 106 p.
- Klimchouk, A.B., 2017. Types and settings of hypogene karst, in hypogene karst regions and caves of the world, In: Klimchouk, A.B., Palmer, A.N., De Waele, J., Auler, A.S., Audra, P. (Eds.), *Hypogene karst regions and caves of the world*. Springer, Cham, p. 1-39. [https://doi.org/10.1007/978-3-319-53348-3\\_1](https://doi.org/10.1007/978-3-319-53348-3_1)
- Koşun, E., Varol, B., Taşkıran, H., 2019. The Antalya Tufas: Landscapes, morphologies, age, formation processes and early human activities. In: Kuzucuoğlu, C., Çiner, A., Kazancı, N. (Eds.), *Landscapes and landforms of Turkey*. World geomorphological landscapes, p. 207-218. [https://doi.org/10.1007/978-3-030-03515-0\\_7](https://doi.org/10.1007/978-3-030-03515-0_7)
- Martin, J.B., Gulley, J., Spellman, P., 2012. Tidal pumping of water between Bahamian blue holes, aquifers, and the ocean. *Journal of Hydrology*, 416, 28-38. <https://doi.org/10.1016/j.jhydrol.2011.11.033>
- McNab, F., Ball, P.W., Hoggard, M.J., White, N.J., 2018. Neogene uplift and magmatism of Anatolia: Insights from drainage analysis and basaltic geochemistry. *Geochemistry, Geophysics, Geosystems*, 19, 175-213 <https://doi.org/10.1002/2017GC007251>
- Mukhin, Y.V., 1965. Processes of compaction of clay sediments. Nedra, Moscow (in Russian).
- Nativ, R., Gunay, G., Hotzl, H., Reichert, B., Solomon, D.K., Tezcan, L., 1999. Separation of groundwater-flow components in a karstified aquifer using environmental tracers. *Applied Geochemistry*, 14, 1001-1014. [https://doi.org/10.1016/S0883-2927\(99\)00012-8](https://doi.org/10.1016/S0883-2927(99)00012-8)
- Okay, A.I., 2008. Geology of Turkey: A synopsis. *Anschnitt*, 21, 19-42.
- Okay, A., Zattin, M., Özcan, E., Sunal, G., 2020. Uplift of Anatolia. *Turkish Journal of Earth Sciences*, 29, 696-713. <https://doi.org/10.3906/yer-2003-10>
- Ozima, M., Podosek, F.A., 1983. Noble gas geochemistry. Cambridge University Press, Cambridge, 367 p.
- Öğretmen, N., Cipollari, P., Frezza, V., Faranda, C., Karanika, K., Gliozzi, E., Radeff, G., Cosentino, D., 2018. Evidence for 1.5 km of uplift of the Central Anatolian Plateau's southern margin in the last 450 kyr and implications for its multiphased uplift history. *Tectonics*, 37, 359-390. <https://doi.org/10.1002/2017TC004805>
- Özgül, N., 1976. Some geological aspects of the Taurus orogenic belt (Turkey). *Bulletin of the Geological Society of Turkey*, 19, 65-78 (in Turkish).
- Özgül, N., 1984. Stratigraphy and tectonic evolution of the Central Tauride. In: Tekeli, O., Göncüoğlu, M.C. (Eds.), *Proceedings of the International Symposium on the Geology of Taurus Belt*, Ankara, p. 77-90.
- Özyurt, N.N., Bayarı, C.S., Tezcan, L., 2000. Groundwater age dating in young groundwater by means of tritium/tritiogenic helium-3 method: Springs of Antalya Travertine Plateau. *Proceedings of the Earth Science and Mining Congress*; Ankara, Turkey. MTA Publications, 557-571 (in Turkish).
- Özyurt, N., 2007. Residence time distribution in the Kirkgoz karst springs (Antalya-Turkey) as a tool for contamination vulnerability assessment. *Environmental Geology*, 53, 1571-1583. <https://doi.org/10.1007/s00254-007-0811-x>
- Özyurt, N.N., Bayarı, C.S., 2014. Helium isotopes as indicator of current hypogenic karst development in Taurids Karst Region, Turkey. In: Klimchouk, A.B., Sasowsky, I., Mylroie, J., Engel, S.A., Engel, A.S. (Eds.), *Selected Papers and Abstracts of the Symposium, Karst Waters Institute Special Publication 18*, Leesburg (VA): Karst Waters Institute, p. 77-81.
- Özyurt, N.N., Bayarı, C.S., 2018. Evolution of noble gas and water isotopes along the regional groundwater flow path of the Konya Closed Basin, Turkey. *International Journal of Speleology*, 47(3), 333-342. <https://doi.org/10.5038/1827-806X.47.3.2176>
- Pekkan, E., 2004. Investigation of the hydrogeochemical processes that affects the formation of obruks as karstic depressions located in the Konya closed basin. Unpublished MSc Thesis, Hacettepe University, Ankara, Turkey, 82 p. (in Turkish).
- Rinehart, J.S., 1976. 18.6-year Earth tide regulates geyser activity. *Science*, 177, 346-347. <https://doi.org/10.1126/science.177.4046.346>
- Schildgen, T.F., Yıldırım, C., Cosentino, D., Strecker, M.R., 2014. Linking slab break-off, Hellenic trench retreat, and uplift of the Central and Eastern Anatolian plateaus. *Earth-Science Reviews*, 128, 147-168 <https://doi.org/10.1016/j.earscirev.2013.11.006>
- Schleiffarth, W.K., Reid, M. R., Darin, M.H., Cosca, M.A., 2016. The Central Anatolian Volcanic Province: Geochronological constraints on the spatiotemporal evolution of volcanism and links to tectonic processes, AGU, Fall Meeting 2016, Abstract.
- Schultz, A., Dickson, P., Elderfield, H., 1996. Temporal variations in diffuse hydrothermal flow at TAG. *Geophysical Research Letters*, 23, 3471-3474. <https://doi.org/10.1029/96GL02081>
- Shestopalov, V.M., 2014. On hydrodynamic zoning and water exchange in hydrogeologic structures. *Geologicheskoy Zhurnal*, 4(349), 9-26 (In Russian). <https://doi.org/10.30836/igs.1025-6814.2014.4.139174>
- Tóth, J., 1963. A theoretical analysis of groundwater flow in small drainage basins. *Journal of Geophysical Research*, 68, 4795-4812. <https://doi.org/10.1029/JZ068i016p04795>
- Tóth, J., 2009. Gravitational systems of groundwater flow: theory, evaluation, utilization. Cambridge University Press, Cambridge. <https://doi.org/10.1017/CBO9780511576546>
- Törk, K.A., 2008. Effect of glaciation phases on the karstification in the Aladaglar mountain range (Nigde-Kayseri-Adana, Turkey), Unpublished PhD Thesis, Hacettepe University, Ankara, Turkey, 153 p. (in Turkish).
- UNDP, 1983. Karst Waters of Southern Turkey, Technical Report, United Nations Development Programme, Report no. DP/UN/TUR-77-015/1, UNDP, New York, 207 p.
- UNESCO, 1972. Glossary and multilingual equivalents of karst terms. Paris, 227 p.
- Valois, R., Rivière, A., Vouillamoz, J.M., Rau, G.C., 2024. Analytical solution for well water response to Earth tides in leaky aquifers with storage and compressibility in the aquitard. *Hydrology and Earth System Sciences*, 28(4), 1041-1054. <https://doi.org/10.5194/hess-28-1041-2024>

Williams, P.W., 1977. Hydrology of the Waikoropupu springs: a major tidal karst resurgence in northwest

Nelson (New Zealand). *Journal of Hydrology*, 35, 73-92.  
[https://doi.org/10.1016/0022-1694\(77\)90078-6](https://doi.org/10.1016/0022-1694(77)90078-6)

© 2024. This work is published under  
<https://creativecommons.org/licenses/by-nc-sa/4.0/legalcode>(the “License”).  
Notwithstanding the ProQuest Terms and Conditions, you may use this  
content in accordance with the terms of the License.